Rotationally Invariant Theory for the Effect of Magnetoelastic Interactions on the Elastic Constants of the Heavy-Rare-Earth Metals*

B. W. Southern and D. A. Goodings
Physics Department, McMaster University, Hamilton, Ontario, Canada
(Received 7 August 1972)

A theory developed by Toupin, Tiersten, Brown, and Melcher employing finite strains and angular-momentum invariants is applied to the rare-earth metals of hcp structure. A Hamiltonian is written down which includes Heisenberg-exchange, crystal field, and magnetoelastic terms and is invariant under combined rotations of the magnetic and elastic systems. When the approximations of small-strain theory are subsequently carried out, there appear new terms originating in the crystal field that are linear in the antisymmetric strains $\omega_{\mu\nu}$ and correspond to rotations of the elastic medium. The coupling of transverse acoustic waves to the magnetic system is studied and expressions are derived for the dependence of the elastic constants c_{44} and c_{66} on an applied magnetic field in the ferromagnetic phase. The terms involving the antisymmetric strains result in new effects similar to those found by Melcher in MnF_2, from which it should be possible to obtain in a direct manner the values of certain magnetoelastic constants and anisotropy constants. Using available data on magnetic anisotropy and magnetostriction, we have estimated the size of the effects that may be expected to be found in Gd, Tb, Dy, Ho, and Er. Fractional changes in c_{44} and c_{66} as large as 10^{-2} are predicted for Tb, Dy, Ho, and Er in a field of about 50 kOe, while the maximum change for Gd is predicted to be about 10^{-4}. Calculations have also been performed for the field-dependent changes in c_{11} and c_{33} for longitudinal waves in the paramagnetic region. These changes result from the fact that the finite strains $E_{\mu\mu}$ include terms of the form $\epsilon_{\mu\mu}^2$. The resulting changes in c_{11} and c_{33} depend linearly on the magnetoelastic constants and vary as H^2 in the paramagnetic region. Estimates of certain combinations of these constants are made from the experimental measurements of Moran and Lüthi on Dy and Ho.

I. INTRODUCTION

A correct description of the physical properties that depend on the coupling between magnetic spins and the lattice in ordered magnetic crystals requires that the Hamiltonian be invariant under a rigid rotation of both the magnetic and elastic systems.[1–4] This condition, which ensures that the total angular momentum of the crystal is conserved, may be satisfied by constructing the Hamiltonian out of certain invariant quantities. The most convenient ones for a microscopic theory are those used by Brown[3] and by Melcher,[4] since they preserve the angular-momentum commutation relations. These are

$$S_{i\mu}^{*}=R_{\mu\nu}S_{i\nu}\ , \tag{1a}$$

$$H_{\mu}^{*}=R_{\mu\nu}H_{\nu}\ , \tag{1b}$$

$$E_{\mu\nu}=\frac{1}{2}\left(\frac{\partial u_\mu}{\partial X_\nu}+\frac{\partial u_\nu}{\partial X_\mu}\right)+\frac{1}{2}\,\frac{\partial u_\lambda}{\partial X_\mu}\,\frac{\partial u_\lambda}{\partial X_\nu}\ , \tag{1c}$$

where $\vec{S}_i$ is the angular momentum of the ith atom and $R_{\mu\nu}$ is an orthogonal tensor which describes a finite rotation of the elastic medium. (For discussions of finite-strain theory, see Brown[3] and Melcher.[5]) The importance of requiring complete rotational invariance has been clearly demonstrated in the antiferromagnetic phase of MnF_2 by Melcher,[6] who was able to account for differences in the elastic constant c_{44} measured as a function of applied magnetic field for transverse waves propagating along the [001] and [110] directions.

In this paper the requirement of rotational invariance is applied to ferromagnetic phases of the rare-earth metals of hcp structure. Expressions are given for the change in elastic constants as a function of applied field for impressed sound waves propagating along different crystal axes. The theory relating to transverse sound waves in the ferromagnetic region is treated in Secs. II and III, and the size of the fractional changes $\Delta c/c$ which can be expected are estimated in Sec. IV for Gd, Tb, Dy, Ho, and Er using the available data on magnetocrystalline anisotropy and magnetostriction. Longitudinal sound waves in the paramagnetic region are discussed in Sec. V.

It seems probable that the measurements of changes in elastic constants proposed in this paper are capable of yielding values for the various magnetoelastic constants and anisotropy constants that are more reliable than those obtained by other methods.

II. THEORY

We take the Hamiltonian for the magnetic spin system of the rare-earth metals of hcp structure to have the form

$$\mathcal{H}_m = -\sum_{i<j} J_{ij}\vec{S}_i^*\cdot\vec{S}_j^* + g\,\mu_B\sum_i \vec{S}_i^*\cdot\vec{H}^* + \tilde{B}_2^0\sum_i \tilde{O}_{20}(\vec{S}_i^*) + \tilde{B}_4^0\sum_i \tilde{O}_{40}(\vec{S}_i^*) + \tilde{B}_6^0\sum_i \tilde{O}_{60}(\vec{S}_i^*) + \tilde{B}_6^6\sum_i [\tilde{O}_{66}(\vec{S}_i^*) + \tilde{O}_{6\,-6}(\vec{S}_i^*)] \quad . \qquad (2)$$

Following the usual custom in this field, $\vec{S}_i$ represents the total (orbital plus spin) angular momentum of ion i, and the $\tilde{O}_{lm}$ are the spin-operator equivalents tabulated by Buckmaster.[7] The terms involving $\tilde{B}_2^0$, $\tilde{B}_4^0$, and $\tilde{B}_6^0$ describe a crystal field of axial symmetry, while the terms involving $\tilde{B}_6^6$ describe a crystal field of hexagonal symmetry.

The single-ion magnetoelastic terms are

$$\mathcal{H}_{me}^{I} = -M_{20}^{\alpha,1}\sum_i E^{\alpha,1}\tilde{O}_{20}(\vec{S}_i^*) - M_{20}^{\alpha,2}\sum_i E^{\alpha,2}\tilde{O}_{20}(\vec{S}_i^*) - M_{21}^{\epsilon}\sum_i\{E_1^{\epsilon}[i\,\tilde{O}_{21}^{+}(\vec{S}_i^*)] + E_2^{\epsilon}[-i\tilde{O}_{21}^{-}(\vec{S}_i^*)]\} - M_{22}^{\gamma}\sum_i [E_1^{\gamma}\tilde{O}_{22}^{+}(\vec{S}_i^*) + E_2^{\gamma}\tilde{O}_{22}^{-}(\vec{S}_i^*)] - M_{44}^{\gamma}\sum_i [E_1^{\gamma}\tilde{O}_{44}^{+}(\vec{S}_i^*) - E_2^{\gamma}\tilde{O}_{44}^{-}(\vec{S}_i^*)] , \qquad (3)$$

where terms corresponding to $l=6$ as well as certain terms corresponding to $l=4$ have been omitted for the sake of simplicity. The operator equivalents $\tilde{O}_{lm}^{\pm}$ are related to those of Buckmaster[7] by

$$\tilde{O}_{lm}^{+} = \tfrac{1}{2}(\tilde{O}_{lm} + \tilde{O}_{l\,-m}) , \qquad (4a)$$

$$\tilde{O}_{lm}^{-} = (1/2i)\,(\tilde{O}_{lm} - \tilde{O}_{l\,-m}) . \qquad (4b)$$

In Eq. (3), the indices α, γ, and ϵ refer to certain combinations of the $E_{\mu\nu}$ which transform according to particular irreducible representations of the point group $6/mmm$.[8] Choosing a coordinate system $(\xi\eta\zeta)$ coinciding with the a, b, and c axes of the crystal, we define

$$E^{\alpha,1} = E_{\xi\xi} + E_{\eta\eta} + E_{\zeta\zeta} , \qquad (5a)$$

$$E^{\alpha,2} = E_{\zeta\zeta} - \tfrac{1}{3}E^{\alpha,1} , \qquad (5b)$$

$$E_1^{\gamma} = \tfrac{1}{2}(E_{\xi\xi} - E_{\eta\eta}) , \qquad (5c)$$

$$E_2^{\gamma} = E_{\xi\eta} , \qquad (5d)$$

$$E_1^{\epsilon} = E_{\eta\zeta} , \qquad (5e)$$

$$E_2^{\epsilon} = E_{\xi\zeta} . \qquad (5f)$$

(As in our earlier paper[9] we have dropped the factor $\frac{1}{2}\sqrt{3}$ from Callen and Callen's definition of $\epsilon^{\alpha,2}$.) The single-ion magnetoelastic terms of Eq. (3) are the same as in our earlier paper,[9] except that the usual symmetric strains $\epsilon_{\mu\nu}$ of small-strain theory have been replaced by the finite-strain tensor $E_{\mu\nu}$, and $S_{i\mu}$ has been replaced by $S_{i\mu}^*$, as required by rotational invariance.[4,5] The coupling constants in (3) are related to those of Callen and Callen[8] by

$$M_{20}^{\alpha,1} = \sqrt{\tfrac{1}{3}}\,\tilde{B}_{12}^{\alpha} , \qquad M_{20}^{\alpha,2} = \sqrt{\tfrac{1}{3}}\,\tilde{B}_{22}^{\alpha} , \qquad M_{21}^{\epsilon} = \sqrt{\tfrac{2}{3}}\,\tilde{B}^{\epsilon} , \qquad M_{22}^{\gamma} = \sqrt{\tfrac{2}{3}}\,\tilde{B}^{\gamma} . \qquad (6)$$

The effect of two-ion magnetoelastic terms will be discussed briefly in Sec. III.

Having ensured complete rotational invariance, we can now carry out the transformation to the usual spin operators $\vec{S}_i$ and the functions

$$\epsilon_{\mu\nu} = \frac{1}{2}\left(\frac{\partial u_\mu}{\partial X_\nu} + \frac{\partial u_\nu}{\partial X_\mu}\right) , \qquad (7a)$$

$$\omega_{\mu\nu} = \frac{1}{2}\left(\frac{\partial u_\mu}{\partial X_\nu} - \frac{\partial u_\nu}{\partial X_\mu}\right) \qquad (7b)$$

of small-strain theory. In addition to the usual terms similar to (2) and (3) with $\vec{S}_i^*$ replaced by $\vec{S}_i$ and $E_{\mu\nu}$ replaced by $\epsilon_{\mu\nu}$ we obtain the following terms linear in the $\omega_{\mu\nu}$:

$$\sqrt{6}\,\tilde{B}_2^0\,\omega_1^{\epsilon}\sum_i (i\,\tilde{O}_{21}^{+}) + \sqrt{6}\,\tilde{B}_2^0\,\omega_2^{\epsilon}\sum_i(-i\,\tilde{O}_{21}^{-}) + 2\sqrt{5}\,\tilde{B}_4^0\,\omega_1^{\epsilon}\sum_i (i\,\tilde{O}_{41}^{+}) + 2\sqrt{5}\,\tilde{B}_4^0\,\omega_2^{\epsilon}\sum_i(-i\,\tilde{O}_{41}^{-}) + \sqrt{42}\,\tilde{B}_6^0\,\omega_1^{\epsilon}\sum_i (i\,\tilde{O}_{61}^{+}) + \sqrt{42}\,\tilde{B}_6^0\,\omega_2^{\epsilon}\sum_i(-i\,\tilde{O}_{61}^{-}) - 12\,\tilde{B}_6^6\,\omega_2^{\gamma}\sum_i \tilde{O}_{66}^{-} + 2\sqrt{3}\,\tilde{B}_6^6\,\omega_1^{\epsilon}\sum_i (i\,\tilde{O}_{65}^{+}) + 2\sqrt{3}\,\tilde{B}_6^6\,\omega_2^{\epsilon}\sum_i (i\,\tilde{O}_{65}^{-}) . \qquad (8)$$

These extra terms, which have not been included in previous studies of the rare-earth metals, involve rotations of the elastic medium and will be found to have a different effect on shear waves propagating in different directions.

Terms of second order in $\epsilon_{\mu\nu}$ and $\omega_{\mu\nu}$ can also be taken into account without difficulty. For transverse waves propagating along one of the crystal axes and polarized along another crystal axis (for which only one of the derivatives $\partial u_\mu/\partial X_\nu$ or $\partial u_\nu/\partial X_\mu$ is nonzero), these terms contribute to the effective elastic constants. However, provided the g tensor is isotropic, as assumed in Eq. (2), these contributions do not depend on the magnetic field in the ferromagnetic phase and consequently do not affect our final results, Eqs. (14)–(16). On the other hand, in the paramagnetic region quadratic terms of the type $\epsilon_{\mu\mu}^2$ give rise to field-dependent changes in the elastic constants for longitudinal waves, resulting from the field-induced magnetization in this region. This will be discussed in Sec. V.

The (unperturbed) magnon energies can now be obtained by standard methods equivalent to the Holstein–Primakoff transformations. It has been found[10–14] that the magnon energies are well represented by a model in which the strains are frozen at their equilibrium values—the so-called "frozen-lattice approximation" of Turov and Shavrov.[15] The magnon energies have the usual form $E_{\vec{q}} = (A_{\vec{q}}^2 - |B_{\vec{q}}|^2)^{1/2}$, with $A_{\vec{q}}$ and $B_{\vec{q}}$ involving the equilibrium strains $\overline{\epsilon}_{\mu\nu}$. The expressions for $A_{\vec{q}}$ and $B_{\vec{q}}$ given by Goodings and Southern[9] for the frozen-lattice approximation remain correct in the present formulation, since in this same approximation $\overline{\omega}_{\mu\nu} = 0$.

The acoustic phonons will be taken to have (unperturbed) energies $\hbar\omega_{\vec{q}\lambda}$, where λ labels the phonon branch.

We now consider the coupling between the acoustic phonons and the magnons, which have two branches in the hcp structure. Provided we consider the coupling to long-wavelength phonons only, this can be derived[16–20] by expressing the displacements u_μ in the strain functions in terms of phonon creation and destruction operators $\beta^\dagger_{\vec{q}\lambda}$ and $\beta_{\vec{q}\lambda}$. Thus we are led to a Hamiltonian of the form

$$\mathcal{H} = \sum_{\vec{q}} E_{\vec{q}} (\alpha^\dagger_{\vec{q}} \alpha_{\vec{q}} + \tfrac{1}{2}) + \sum_{\vec{q}\lambda} \hbar\omega_{\vec{q}\lambda} (\beta^\dagger_{\vec{q}\lambda} \beta_{\vec{q}\lambda} + \tfrac{1}{2})$$

$$+ \sum_{\vec{q}\lambda} [V_{\vec{q}\lambda} \alpha_{\vec{q}} (\beta^\dagger_{\vec{q}\lambda} + \beta_{-\vec{q}\lambda}) + V^*_{\vec{q}\lambda} \alpha^\dagger_{\vec{q}} (\beta_{\vec{q}\lambda} + \beta^\dagger_{-\vec{q}\lambda})] . \quad (9)$$

The detailed derivation of (9) yields no coupling between the acoustic phonons of long wavelength and the higher-energy magnon mode, and consequently we have included in (9) only the lower magnon branch with creation and destruction operators $\alpha^\dagger_{\vec{q}}$ and $\alpha_{\vec{q}}$. The expressions for the $V_{\vec{q}\lambda}$ are very lengthy even for the incomplete Hamiltonian considered here. Allowing for differences in notation, our results agree with those given by Nayyar and Sherrington,[20] except that there are additional terms involving the anisotropy constants which come from Eq. (8). The full expressions are given in the Appendix.

We have not included in Eq. (9) terms of the type considered by Jensen[18] involving products of two magnon operators and one phonon operator. These will be unimportant at low temperatures but might become appreciable close to T_c. Equations of motion for the operators $\alpha^\dagger_{\vec{q}}$, $\alpha_{-\vec{q}}$, $\beta^\dagger_{\vec{q}\lambda}$, and $\beta_{-\vec{q}\lambda}$ may be written down using the Hamiltonian (9), and since the eight equations are linear, the coupled-mode frequencies are in general the roots of an eighth-order equation. However, if we confine our attention to the coupling between the lower magnon branch and an impressed sound wave which has a definite direction of propagation and a definite polarization along one of the crystal axes, then the coupled-mode energies can be shown to be

$$\epsilon^2_{\vec{q}\lambda} = \tfrac{1}{2}(E^2_{\vec{q}} + \hbar^2\omega^2_{\vec{q}\lambda}) \pm \tfrac{1}{2}[(E^2_{\vec{q}} - \hbar^2\omega^2_{\vec{q}\lambda})^2 + 16 E_{\vec{q}} \hbar\omega_{\vec{q}\lambda} |V_{\vec{q}\lambda}|^2]^{1/2} , \quad (10)$$

where $\vec{q}$ gives the direction of propagation and λ the branch or polarization of the impressed sound wave. Where the unperturbed magnon and phonon curves would have intersected, there are gaps of magnitude $2|V_{\vec{q}\lambda}|$.[18–20] We shall be concerned only with the behavior at long wavelengths where, assuming $E_0 \neq 0$, we have $\hbar\omega_{\vec{q}\lambda} \ll E_{\vec{q}}$. The lower coupled-mode energy in this limit is given by

$$\epsilon^2_{\vec{q}\lambda} = \hbar^2\omega^2_{\vec{q}\lambda} - \frac{4\hbar\omega_{\vec{q}\lambda} |V_{\vec{q}\lambda}|^2}{E_{\vec{q}}} . \quad (11)$$

Note added in proof. Chow and Keffer (to be published) have obtained the same expression as Eq. (10) for the energy of the coupled modes, and, in the case of weak coupling between the magnons and phonons, they obtain Eq. (11) for the lower coupled-mode energy.

If we define an effective elastic constant c^* by the relation

$$(\epsilon_{\vec{q}\lambda}/\hbar)^2 = (c^*/\rho)|\vec{q}|^2 , \quad (12)$$

where ρ is the density, then c^* may be derived for various types of impressed sound waves and different directions of the applied magnetic field. Since the results for an arbitrary orientation of the applied field are complicated, we shall quote only the results for $\vec{H}$ parallel to one of the crystal axes. Expressions for the general case can be obtained using the equations of the Appendix.

An important assumption of the results that follow [Eqs. (14)–(16)] is that the magnetization has been brought into the direction of the applied field, and we denote by H_0 a field large enough both to overcome the effects of magnetocrystalline anisotropy and to give nearly complete alignment of domains. It appears from the recent paper by Palmer and Lee[21] on the elastic constants of Dy and Ho that changes in the elastic constants due to domain effects can be of the order of 1% and consequently can mask the "intrinsic" field dependence with which we are concerned. Another instance is the dip in c_{33} as a function of temperature measured by Long, Wazzan, and Stern[22] in Gd near 220 K. This has been interpreted by Levinson and Shtrikman[23] as essentially arising from the alignment of domains below about 5 kOe. Thus it is important that H_0 be large enough to achieve complete saturation of the magnetization in the direction of the applied field. The minimum value of H_0 will also depend on the demagnetizing fields in the sample. For example, in a Gd crystal of rectangular cross section, Moran and Lüthi[24] found that the magnetization did not saturate until $H = 10$ kOe.

Below we give our results for the changes in elastic constants as a function of magnetic field based on Eqs. (11) and (12) and the preceding theory. The case in which the field is applied along the c axis and the case in which it is applied along either an a or b axis will be considered separately. It is convenient to introduce the following definitions, with N_a the number of atoms per unit volume:

$$b_2 = N_a \tilde{B}_2^0 SS(\tfrac{1}{2}) , \tag{13a}$$

$$b_4 = N_a \tilde{B}_4^0 SS(\tfrac{3}{2}) , \tag{13b}$$

$$b_6 = N_a \tilde{B}_6^0 SS(\tfrac{5}{2}) , \tag{13c}$$

$$b_6^6 = N_a \tfrac{1}{16}(231)^{1/2} \tilde{B}_6^6 SS(\tfrac{5}{2}) , \tag{13d}$$

$$b_2^\epsilon = N_a (\tfrac{3}{2})^{1/2} M_{21}^\epsilon SS(\tfrac{1}{2}) = \tfrac{1}{2} c^\epsilon H(0) , \tag{13e}$$

$$b_2^\gamma = N_a (\tfrac{3}{2})^{1/2} M_{22}^\gamma SS(\tfrac{1}{2}) = 2c^\gamma C(0) , \tag{13f}$$

$$b_4^\gamma = N_a (\tfrac{70}{16})^{1/2} M_{44}^\gamma SS(\tfrac{3}{2}) = -2c^\gamma A(0) , \tag{13g}$$

$$S(n) = (S-\tfrac{1}{2})(S-1)\cdots(S-n) , \tag{13h}$$

$$h = N_a g \mu_B HS , \tag{13i}$$

$$h_0 = N_a g \mu_B H_0 S . \tag{13j}$$

The constants $H(0)$, $C(0)$, and $A(0)$ occurring in (13e)–(13g) are the magnetostriction constants of Mason[25] at $T=0$. Also, $c^\epsilon = 4c_{44}$ and $c^\gamma = 4c_{66}$.

Case 1. *H parallel to c axis.* In this case, c_{11}, c_{33}, and c_{66} are not affected by the applied field in the ferromagnetic region. For the field dependence of c_{44}, we find

$$c_{44}^*(H) - c_{44}^*(H_0) = \frac{m(h-h_0)(b_2^\epsilon m^3 \pm f_1)^2}{4(f_1+mh_0)(f_1+mh)} , \tag{14a}$$

where

$$f_1 = -3b_2 m^3 - 10 b_4 m^{10} - 21 b_6 m^{21} . \tag{14b}$$

Here $m = M(T)/M(0)$ is the reduced magnetization. The upper sign in (14a) is the result for a wave propagating along the c axis and polarized along either the a or b direction, while the lower sign is for propagation along either the a or b axis and polarized in the c direction. The usual small-strain theory yields the same result for both types of wave, the last factor in the numerator of (14a) being simply $(b_2^\epsilon m^3)^2$.

It may be appropriate to mention at this point that an expression for the magnetoelastic contribution to c_{44} has been obtained by Freyne[26] within the framework of molecular-field theory. His result varies as $(b_2^\epsilon)^2$ divided by the energy of the molecular field, in contrast to the present work in which we obtain $(b_2^\epsilon)^2$ divided by the anisotropy energy in the form of (14b). Since in the case of Gd the energy of the molecular field is at least 100 times larger than the anisotropy energy, it follows that Freyne's predictions are approximately 100 times smaller than ours. (Note, however, that his estimates become multiplied at a later stage by a factor of 200, which represents approximately the number of terms appearing in his expression for the internal energy.)

Case 2. *H parallel to a or b axis.* In this case, c_{11} and c_{33} are not affected by the applied field in the ferromagnetic region. The behavior of c_{44} is given by

$$c_{44}^*(H) - c_{44}^*(H_0) = \frac{m(h-h_0)[b_2^\epsilon m^3 \mp f_2(\tfrac{1}{2}\pi)]^2}{4[f_2(\tfrac{1}{2}\pi)+mh_0][f_2(\tfrac{1}{2}\pi)+mh]} , \tag{15a}$$

where

$$f_2(\tfrac{1}{2}\pi) = 3b_2 m^3 - \tfrac{15}{2} b_4 m^{10} + \tfrac{105}{8} b_6 m^{21} - 6b_6^6 \cos 6\phi\, m^{21} + (4c^\gamma)^{-1}[2(b_2^\gamma m^3)^2 + (b_4^\gamma m^{10})^2 + 3(b_2^\gamma m^3)(b_4^\gamma m^{10})\cos 6\phi] . \tag{15b}$$

Here ϕ is zero for $\vec{H} \parallel \vec{a}$ and $\tfrac{1}{2}\pi$ for $\vec{H} \parallel \vec{b}$. The upper sign in (15a) is the result for a sound wave propagating along the c axis and polarized along the direction of $\vec{H}$. The lower sign is for propagation along the direction of $\vec{H}$ and polarized along the c axis. Again the small-strain theory gives the same result for both types of wave, the last factor in the numerator of (15a) being simply $(b_2^\epsilon m^3)^2$.

For transverse waves propagating in the a or b directions and polarized in the basal plane, we find the result

$$c_{66}^*(H) - c_{66}^*(H_0) = \frac{m(h-h_0)[b_c^\gamma(\tfrac{1}{2}\pi) \mp f_3(\tfrac{1}{2}\pi)]^2}{4[f_3(\tfrac{1}{2}\pi)+mh_0][f_3(\tfrac{1}{2}\pi)+mh]} , \tag{16a}$$

where

$$f_3(\tfrac{1}{2}\pi) = -36 b_6^6 \cos 6\phi\, m^{21} + (4c^\gamma)^{-1}[4(b_2^\gamma m^3)^2 + 4(b_4^\gamma m^{10})^2 + 10(b_2^\gamma m^3)(b_4^\gamma m^{10})\cos 6\phi] , \tag{16b}$$

$$b_c^\gamma(\tfrac{1}{2}\pi) = b_2^\gamma m^3 \cos 2\phi - b_4^\gamma m^{10} \cos 4\phi . \tag{16c}$$

The upper sign in (16a) is the result for propagation along the a direction while polarized in the b direction, and the lower sign is for propagation along the b direction while polarized in the a direction. ϕ is zero for $\vec{H} \parallel \vec{a}$ and $\tfrac{1}{2}\pi$ for $\vec{H} \parallel \vec{b}$. Small-strain theory results in the same expression for both types of wave, the last factor in the numerator of (16a) being simply $[b_c^\gamma(\tfrac{1}{2}\pi)]^2$ for either orientation of the applied field.

Although we have obtained these results from the

Hamiltonian in the form of Eq. (9), we have verified for case 1 that the same results are obtained by solving the macroscopic equations for the transverse components of magnetization and the elastic displacements, having first rewritten the Hamiltonian of Eqs. (2) and (3) together with the elastic energy in terms of macroscopic quantities. In this case, in which the spins are aligned along the c axis, the calculation for the present two-sublattice ferromagnet is only slightly different from that carried out by Melcher[5,6] for the two-sublattice uniaxial antiferromagnet.

III. EFFECT OF TWO-ION MAGNETOELASTIC INTERACTIONS

In addition to the one-ion magnetoelastic terms of Eq. (3) there occur two-ion magnetoelastic terms which come primarily from the strain dependence of the exchange interactions. In this section we examine briefly how the inclusion of these terms affects the results of Sec. II (and the Appendix).

To second order in the angular-momentum invariants $S^*_{i\mu}$ and first order in the finite strains $E_{\mu\nu}$, the two-ion terms are[8,9]

$$\mathcal{H}^{\mathrm{II}}_{\mathrm{me}} = \sum_{i<j} \mathcal{H}^{\mathrm{II}}_{\mathrm{me}}(i,j)\ , \tag{17a}$$

$$\begin{aligned}\mathcal{H}^{\mathrm{II}}_{\mathrm{me}}(i,j) = &-\tilde{D}^{\alpha}_{11\,ij} E^{\alpha,1} \vec{S}^*_i\cdot\vec{S}^*_j - \tilde{D}^{\alpha}_{12\,ij} E^{\alpha,1} (\tfrac{1}{2}\sqrt{3})(S^{\zeta *}_i S^{\zeta *}_j - \tfrac{1}{3}\vec{S}^*_i\cdot\vec{S}^*_j) - \tilde{D}^{\alpha}_{21\,ij} E^{\alpha,2} \vec{S}^*_i\cdot\vec{S}^*_j \\ &- \tilde{D}^{\alpha}_{22\,ij} E^{\alpha,2} (\tfrac{1}{2}\sqrt{3})(S^{\zeta *}_i S^{\zeta *}_j - \tfrac{1}{3}\vec{S}^*_i\cdot\vec{S}^*_j) - \tilde{D}^{\gamma}_{ij}[E^{\gamma}_1 \tfrac{1}{2}(S^{\xi *}_i S^{\xi *}_j - S^{\eta *}_i S^{\eta *}_j) + E^{\gamma}_2 \tfrac{1}{2}(S^{\xi *}_i S^{\eta *}_j + S^{\eta *}_i S^{\xi *}_j)] \\ &- \tilde{D}^{\epsilon}_{ij}[E^{\epsilon}_1 \tfrac{1}{2}(S^{\eta *}_i S^{\zeta *}_j + S^{\zeta *}_i S^{\eta *}_j) + E^{\epsilon}_2 \tfrac{1}{2}(S^{\xi *}_i S^{\zeta *}_j + S^{\zeta *}_i S^{\xi *}_j)]\ .\end{aligned} \tag{17b}$$

The main way in which these affect the results of Sec. II is to cause the following replacements wherever they occur in Eqs. (14)–(16) and in the equations of the Appendix:

$$b^{\gamma}_2 m^3 \rightarrow b^{\gamma}_2 m^3 + d^{\gamma} m^2\ , \tag{18a}$$

$$b^{\epsilon}_2 m^3 \rightarrow b^{\epsilon}_2 m^3 + d^{\epsilon} m^2\ , \tag{18b}$$

where

$$d^{\gamma} = \tfrac{1}{2} N_a S^2 \sum_j \tilde{D}^{\gamma}_{ij}\ , \tag{19a}$$

$$d^{\epsilon} = \tfrac{1}{2} N_a S^2 \sum_j \tilde{D}^{\epsilon}_{ij}\ . \tag{19b}$$

In the latter definitions the sum over j is over all neighbors of i, not just those on one sublattice.

In practice it will be difficult to separate these one- and two-ion magnetoelastic contributions, since their temperature dependence is quite similar. In the calculations to be described in Sec. IV we have regarded the two-ion terms as making effective contributions to $b^{\gamma}_2 m^3$ and $b^{\epsilon}_2 m^3$, the size of which is unknown. However, since the strain dependence of the Heisenberg exchange terms and the simplest anisotropic exchange terms leads only to terms of α symmetry in (17), the two-ion terms in d^{γ} and d^{ϵ} must have their origin in some higher-order coupling between the angular momenta $\vec{S}_i$ and $\vec{S}_j$, and thus there is reason to believe that they will be much smaller than b^{γ}_2 and b^{ϵ}_2.

IV. ESTIMATES FOR Gd, Tb, Dy, Ho, AND Er

Measurements of the changes in elastic constants as a function of the applied field can be analyzed using the expressions of Sec. III in order to obtain accurate values of the various magnetoelastic constants and, in favorable cases, of the anisotropy

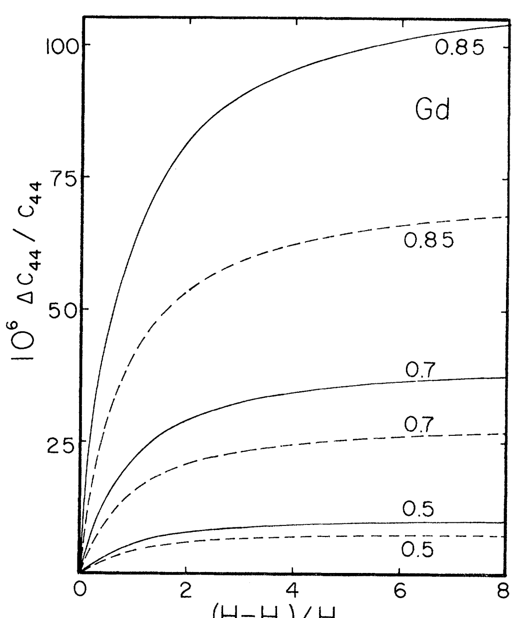

FIG. 1. $\Delta c_{44}/c_{44}$ as a function of $(H-H_0)/H_0$ for Gd calculated from Eq. (15a) for a magnetic field along the a axis. $H_0 = 10$ kOe, $b^{\epsilon}_2 = 0.54\times10^8$ ergs/cm^3, and $c_{44} = 0.226\times10^{12}$ ergs/cm^3. Solid curves are for propagation along the c axis and dashed curves are for propagation along the a axis. Curves are shown for values of the reduced magnetization m ranging from 0.85 to 0.5.

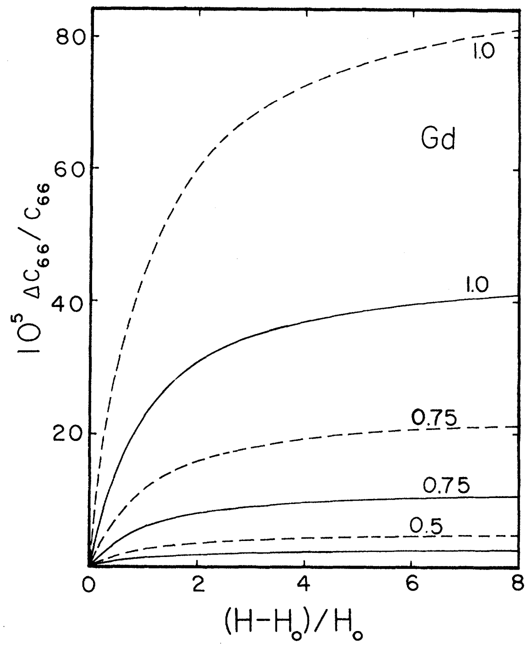

FIG. 2. $\Delta c_{66}/c_{66}$ as a function of $(H-H_0)/H_0$ for Gd calculated from Eq. (16a) for a magnetic field along the a axis. $b_2^\gamma = 0.92\times 10^8$ ergs/cm^3 and $c_{66}=0.229\times 10^{12}$ ergs/cm^3. The dashed curves are for $H_0=5$ kOe, while the solid curves are for $H_0=10$ kOe. Curves are shown for values of m ranging from 1.0 to 0.5.

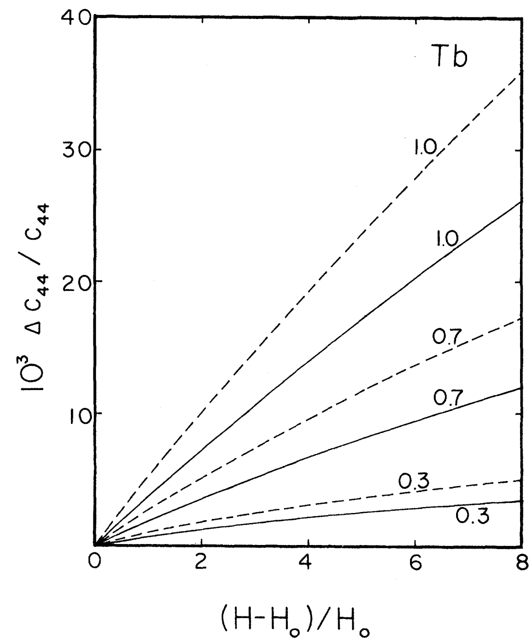

FIG. 3. $\Delta c_{44}/c_{44}$ as a function of $(H-H_0)/H_0$ for Tb calculated from Eq. (15a) for a magnetic field along the b axis. $H_0=10$ kOe, $b_2^\epsilon=180\times 10^8$ ergs/cm^3, and $c_{44}=0.228\times 10^{12}$ ergs/cm^3. Solid curves are for propagation along the c axis and dashed curves are for propagation along the direction of the magnetic field. Curves are shown for values of m ranging from 1.0 to 0.3.

constants as well. In this section we turn this process around and use the available data for the magnetoelastic constants and the anisotropy constants to estimate the size of the effects which can be expected to be measured experimentally. The discussion is restricted, of course, to temperature ranges in which ferromagnetism occurs, the temperature dependence having been expressed through powers of the reduced magnetization in Secs. II and III. In fact, in making the estimates that follow we have replaced $m^{l(l+1)/2}$ by the (normalized) hyperbolic Bessel function $\hat{I}_{l+1/2}(\mathcal{L}^{-1}(m))$ in order to improve the results in the region of higher temperatures.[27] Throughout this section we shall be concerned with transverse acoustic waves only. Longitudinal waves will be treated in Sec. V.

TABLE I. Estimates of the anisotropy constants b_2, b_4, b_6, b_6^6, and the magnetic field parameter h corresponding to $H=10$ kOe.

	N_a $\left(10^{22}\ \frac{\text{atoms}}{\text{cm}^3}\right)$	b_2 $\left(10^6\ \frac{\text{ergs}}{\text{cm}^3}\right)$	b_4 $\left(10^6\ \frac{\text{ergs}}{\text{cm}^3}\right)$	b_6 $\left(10^6\ \frac{\text{ergs}}{\text{cm}^3}\right)$	b_6^6 $\left(10^6\ \frac{\text{ergs}}{\text{cm}^3}\right)$	Ref.	h for $H=10$ kOe $\left(10^6\ \frac{\text{ergs}}{\text{cm}^3}\right)$
Gd	3.04	−1.3	+0.69		−0.0064	28, 29	19.7
	3.04	−0.55	+0.64	−0.061	−0.0064	30, 31	19.7
Tb	3.15	+565	+46		+1.85	28	26.3
	3.15	+550			+2.42	32	26.3
	3.15	+450				33	26.3
Dy	3.17	+550	−54		−11	28	29.4
	3.17	+550			−7.6	32	29.4
	3.17	+490				33	29.4
Ho	3.21	+416	+177		+27	28	29.8
	3.21	+63	+48		+0.21	34	29.8
Er	3.26	−180[a]	−27[a]	+62[a]	−38[a]	35	27.2

[a]Deduced from analysis of HoEr alloys.

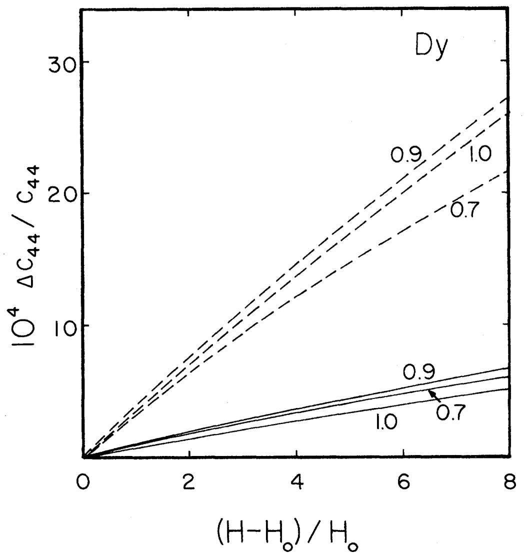

FIG. 4. Same curves for Dy as in Fig. 3 except that the magnetic field is along the a axis. $b_2^{\epsilon}=56\times 10^8$ ergs/cm^3 and $c_{44}=0.257\times 10^{12}$ ergs/cm^3.

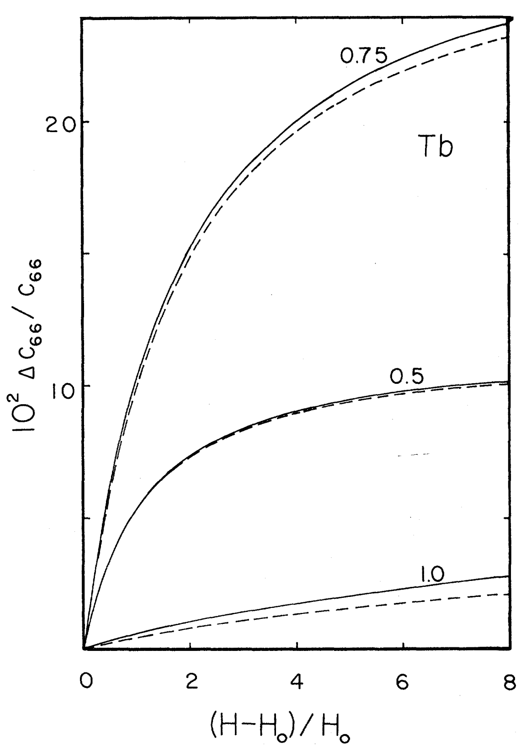

FIG. 5. $\Delta c_{66}/c_{66}$ as a function of $(H-H_0)/H_0$ for Tb calculated from Eq. (16a) for a magnetic field along the b axis. $H_0=10$ kOe, $b_2^{\gamma}=77\times 10^8$ ergs/cm^3, $b_4^{\gamma}=-41\times 10^8$ ergs/cm^3, and $c_{66}=0.22\times 10^{12}$ ergs/cm^3. Solid curves are for propagation along the a axis and dashed curves are for propagation along the b axis. Curves are shown for values of m ranging from 1.0 to 0.5.

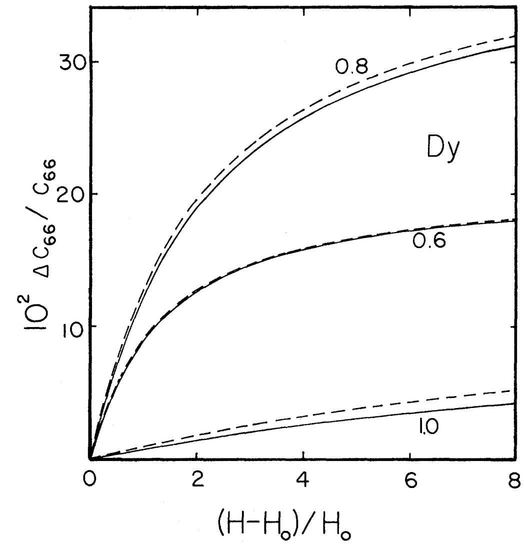

FIG. 6. Same curves for Dy as in Fig. 5 except that the magnetic field is along the a axis. $b_2^{\gamma}=89\times 10^8$ ergs/cm^3, $b_4^{\gamma}=0$, and $c_{66}=0.263\times 10^{12}$ ergs/cm^3.

Estimates of the various anisotropy constants obtained from torque measurements and magnetization curves are given in Table I for Gd, Tb, Dy, Ho, and Er. The values used in the calculations of Figs. 1–7 were those determined from magnetiza-

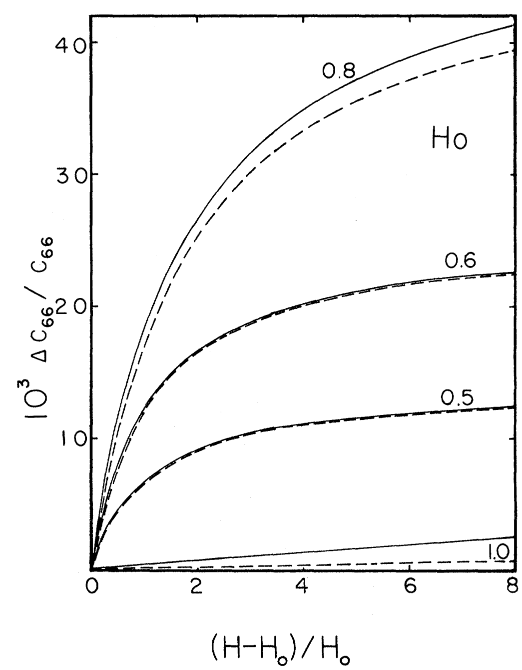

FIG. 7. $\Delta c_{66}/c_{66}$ as a function of $(H-H_0)/H_0$ for Ho calculated from Eq. (16a) for a magnetic field along the b axis. $H_0=10$ kOe, $b_2^{\gamma}=31\times 10^8$ ergs/cm^3, $b_4^{\gamma}=0$, and $c_{66}=0.308\times 10^{12}$ ergs/cm^3. Solid curves are for propagation along the a axis and dashed curves are for propagation along the b axis. Curves are shown for values of m ranging from 1.0 to 0.5.

TABLE II. Estimates of b_2^ϵ.

	c_{44} $\left(10^{12}\ \frac{\text{ergs}}{\text{cm}^3}\right)$	Temp. of measurement (K)	Ref.	$\lambda^\epsilon(0)$ (10^{-3})	Ref.	$b_2^\epsilon = 4c_{44}\lambda^\epsilon(0)$ $10^8\left(\frac{\text{ergs}}{\text{cm}^3}\right)$
Gd	0.238	4	36	0.04	40	0.57
	0.213	300	37	0.04	40	0.51
Tb	0.228	300	37	20	41	180
Dy	0.270	0	38	9.16	42	59.4
	0.243	298	39	9.16	42	53.5

tion curves by Feron, Hug, and Pauthenet.[28] Tables II and III give estimates of b_2^ϵ, b_2^γ, and b_4^γ based on the available magnetostrictive data.

A. Gadolinium

Figure 1 shows the estimated fractional change in the elastic constant c_{44} for a magnetic field along the a axis. The ordinate is $[c_{44}^*(H) - c_{44}^*(H_0)]/c_{44}^*$ calculated from Eq. (15a), it being immaterial what strength of H is used for c_{44}^* in the denominator. A value of $H_0 = 10$ kOe was chosen, which is probably large enough to saturate the magnetization and sufficient to mask the undesirable effect of nonuniform demagnetizing fields in nonellipsoidal samples. The solid curves are the results for transverse waves propagating along the c axis and polarized in the a direction, while the dashed curves are for waves propagating along the a axis and polarized in the c direction. Our calculations show that as m decreases from 1.0 to 0.3, $\Delta c_{44}/c_{44}$ decreases by about two orders of magnitude. Thus the most accurate values of b_2^ϵ will be obtained from measurements at low temperatures. A detailed study of the temperature dependence of the results might also yield values of the anisotropy constants b_2 and b_4 contained in the function $f_2(\frac{1}{2}\pi)$.

Estimates of the fractional change in c_{66} based on Eq. (16a) for a field H along the a axis are shown in Fig. 2. The results for transverse waves propagating along the a or b axis and polarized in the plane are indistinguishable from each other as a consequence of the weak hexagonal anisotropy. To show the effect of choosing different values for the minimum field H_0, curves have been plotted for $H_0 = 5$ and 10 kOe with m ranging from 1.0 to 0.5. Again the greatest fractional change is expected at low temperatures.

It is worth noting that measurements of $\Delta c_{66}/c_{66}$ for $\vec{H} \parallel \vec{b}$ when compared with the results for $\vec{H} \parallel \vec{a}$ provide the possibility of obtaining independent values for b_2^γ and b_4^γ, as may be seen from Eqs. (16), setting $\phi = \frac{1}{2}\pi$ and $\phi = 0$ in the two cases.

B. Terbium and Dysprosium

Since the anisotropy constants and magnetoelastic constants for Tb and Dy are about two orders of magnitude larger than for Gd, the fractional changes in elastic constants $\Delta c/c$ are of order $10^{-3} - 10^{-2}$ compared with about 10^{-5}–10^{-4} in the case of Gd.[24] Figures 3 and 4 show calculations of $\Delta c_{44}/c_{44}$ for Tb and Dy, respectively, based on Eq. (15a). The magnetic field was taken to be along the easy direction (b axis for Tb, a axis for Dy) and H_0 was chosen to be 10 kOe in each case. The solid curves are for waves propagating along the c axis and polarized in the easy direction, while the dashed curves are for waves propagating along the easy direction and polarized in the c direction. In comparison with Gd, these curves are much more nearly linear because the anisotropy terms dominate the effect of the field in the denominator of Eq. (15a). For Tb the largest fractional changes occur at low temperatures, while for Dy the largest changes occur in the region of $m = 0.85$ as a result of a competition among the various factors in the numerator and denominator of Eq. (15a).

In Figures 5 and 6 we have plotted estimates of $\Delta c_{66}/c_{66}$ for Tb and Dy, respectively, based on Eq. (16a). The magnetic field was taken to be along the easy direction in each case and H_0 was

TABLE III. Estimates of b_2^γ and b_4^γ.

	c_{66} $\left(10^{12}\ \frac{\text{ergs}}{\text{cm}^3}\right)$	Temp. of measurement (K)	Ref.	$\lambda^{\gamma,2}(0) = 2C(0)_{\text{Mason}}$ (10^{-3})	$\lambda^{\gamma,4}(0) = -2A(0)_{\text{Mason}}$ (10^{-3})	Ref.	$b_2^\gamma = 4c_{66}\lambda^{\gamma,2}(0)$ $\left(10^8\ \frac{\text{ergs}}{\text{cm}^3}\right)$	$b_4^\gamma = 4c_{66}\lambda^{\gamma,4}(0)$ $\left(10^8\ \frac{\text{ergs}}{\text{cm}^3}\right)$
Gd	0.229	4	36	0.10		40	0.92	
Tb	0.22	...	43	8.7	−4.3	45	77	−38
	0.22	...	43	8.5	−5.0	41	76	−44
Dy	0.283	0	38	8.5		42	96	
	0.243	298	39	8.5		42	82	
Ho	0.308[a]	4	44	2.5		46	31	
Er	0.303	63	39	−5.4		47	−65	
	0.279	298	39	−5.4		47	−60	

[a]Shear modulus measured in a polycrystalline sample.

chosen to be 10 kOe. The solid curves are for propagation along the a axis polarized in the b direction, while the dashed curves have these two directions interchanged. The small difference between these two sets of curves results from the fact that the hexagonal anisotropy is at least 20 times smaller than $b_c(\frac{1}{2}\pi)$ near $T=0$. As $f_3(\frac{1}{2}\pi)$ falls to zero with increasing temperature, the two sets of curves become indistinguishable. It can be seen from Figs. 5 and 6 that the maximum changes in c_{66} occur around $m=0.75$. The fact that the largest changes do not occur at the lowest temperatures is due to the denominator of Eq. (16a) decreasing rapidly as m decreases from 1.0 until, when m is about 0.8, the function $f_3(\frac{1}{2}\pi)$ becomes comparable with mh_0. The curvature of the curves other than $m=1.0$ is also due to the function $f_3(\frac{1}{2}\pi)$ having fallen nearly to zero so that only the magnetic field term is appreciable in the denominator of (16a). In the case of Tb the curve for $m=1.0$ is further depressed because the competition between b_2^γ and b_4^γ produces a maximum in $b_c^\gamma(\frac{1}{2}\pi)$ near $m=0.92$.

C Holmium and Erbium

Since there are no magnetoelastic data from which to estimate b_2^ϵ for holmium and erbium, it is not possible to predict the size of $\Delta c_{44}/c_{44}$ for these metals. Measurements of appropriate sound velocities should yield reliable estimates of this coupling constant and perhaps of the anisotropy constants as well. It may be seen in Table I that there is a considerable difference between the values of b_2 and b_4 for Ho obtained from the work of Feron *et al.*[28] and from Bozorth *et al.*[34]

In Fig. 7 we have plotted estimates of $\Delta c_{66}/c_{66}$ for Ho based on Eq. (16a) using $b_6^6=27\times10^6$ ergs/cm^3, the value deduced by Feron *et al.*[28] The solid curves are for waves propagating along the a direction and polarized in the b direction, while the dashed curves have these two directions interchanged. The magnetic field was taken to be along the easy direction (b axis) and H_0 was chosen to be 10 kOe. As for Tb and Dy, the greatest change occurs in the region $m=0.75$ as a result of $f_3(\frac{1}{2}\pi)$ falling rapidly to zero with decreasing m in Eq. (16a). Rather similar results are obtained for Er using the parameter values given in Tables I and III, but the scale of the curves is increased by a factor of about 3.5. This is mainly due to the fact that b_2^γ is about twice as large for Er compared with Ho.

If the very much smaller value of $b_6^6=0.21\times10^6$ ergs/cm^3 for Ho due to Bozorth *et al.*[34] is used in the calculations, then the function $f_3(\frac{1}{2}\pi)$ in Eq. (16a) is almost negligible and the denominator of (16a) depends almost entirely on the magnetic field terms mh and mh_0. The result is that the greatest fractional change in c_{66} occurs for $m=1.0$, with a value about 3.5 times the maximum in Fig. 7. Thus the magnitude of the change is rather sensitive to the value of b_6^6. When b_6^6 is small, it is also sensitive to the choice of H_0.

V. LONGITUDINAL WAVES IN PARAMAGNETIC REGION

As discussed in Sec. II, the requirement of rotational invariance and the use of the finite-strain tensor led to additional magnetoelastic terms linear in the antisymmetric strains $\omega_{\mu\nu}$. For the case of longitudinal sound waves, there occur other terms quadratic in the infinitesimal strains $\epsilon_{\mu\mu}$ which arise entirely from the definition of the finite strains. From Eq. (1) we have for a pure longitudinal wave

$$E_{\mu\mu}=\epsilon_{\mu\mu}+\tfrac{1}{2}\epsilon_{\mu\mu}^2 . \quad (20)$$

(The summation convention does not apply to this equation.) When these are retained in the single-ion magnetoelastic Hamiltonian (3), with the term in M_{44}^γ neglected, and thermal averages of spin operators are taken, we obtain the following expressions for the changes in elastic constants:

$$\Delta c_{33}=-(b_1^\alpha+\tfrac{2}{3}b_2^\alpha)P_2^0(\cos\theta)\langle\tilde{O}_{20}\rangle/SS(\tfrac{1}{2}) , \quad (21a)$$

$$\Delta c_{11}=-(b_1^\alpha-\tfrac{1}{3}b_2^\alpha)P_2^0(\cos\theta)\langle\tilde{O}_{20}\rangle/SS(\tfrac{1}{2}) \mp\tfrac{1}{4}b_2^\gamma\sin^2\theta\cos2\phi\langle\tilde{O}_{20}\rangle/SS(\tfrac{1}{2}) , \quad (21b)$$

where b_1^α and b_2^α are defined by

$$b_1^\alpha=N_a M_{20}^{\alpha,1}SS(\tfrac{1}{2}) , \quad (22a)$$

$$b_2^\alpha=N_a M_{20}^{\alpha,2}SS(\tfrac{1}{2}) . \quad (22b)$$

In Eq. (21b) the upper sign is for propagation along the a axis and the lower sign is for propagation along the b axis. The thermal averages $\langle\tilde{O}_{20}\rangle$ are to be taken with respect to the equilibrium spin direction, which is specified by (θ,ϕ). In the ferromagnetic region at low temperatures $\langle\tilde{O}_{20}\rangle/SS(\frac{1}{2})$ reduces to m^3 in the usual way.[9] However, in the paramagnetic region when $m(T,H)\ll1$, one can use the approximate relation[8,24]

$$\langle\tilde{O}_{20}\rangle\approx\tfrac{3}{5}\,SS(\tfrac{1}{2})[m(T,H)]^2 . \quad (23)$$

Introducing the susceptibility $\chi(T)$ through

$$M(T,H)=\chi(T)H , \quad (24)$$

we have

$$\langle\tilde{O}_{20}\rangle\approx\tfrac{3}{5}\,SS(\tfrac{1}{2})[\chi(T)/M(T=0)]^2H^2 . \quad (25)$$

This is to be substituted in Eqs. (21a) and (21b) to obtain the changes Δc_{33} and Δc_{11} in the paramagnetic region.

The effect of two-ion magnetoelastic terms may be included by considering the Hamiltonian in Eqs. (17) and retaining terms which arise from the quadratic terms in (20). The changes in elastic constants become

$$\Delta c_{33} = \{ -\tfrac{3}{5}(b_1^\alpha + \tfrac{2}{3} b_2^\alpha) P_2^0(\cos\theta) - (d_{11}^\alpha + \tfrac{2}{3} d_{21}^\alpha) - (d_{12}^\alpha + \tfrac{2}{3} d_{22}^\alpha) P_2^0(\cos\theta)\} [\chi(T)/M(T=0)]^2 H^2 , \tag{26a}$$

$$\Delta c_{11} = [-\tfrac{3}{5}(b_1^\alpha - \tfrac{1}{3} b_2^\alpha) P_2^0(\cos\theta) - (d_{11}^\alpha - \tfrac{1}{3} d_{21}^\alpha) - (d_{12}^\alpha - \tfrac{1}{3} d_{22}^\alpha) P_2^0(\cos\theta) \mp \tfrac{1}{4}(\tfrac{3}{5} b_2^\gamma + d^\gamma) \times \sin^2\theta \cos 2\phi] [\chi(T)/M(T=0)]^2 H^2 , \tag{26b}$$

where the following definitions have been used:

$$d_{11}^\alpha = N_a S^2 \tfrac{1}{2} \sum_j \tilde{D}_{11ij}^\alpha , \tag{27a}$$

$$d_{21}^\alpha = N_a S^2 \tfrac{1}{2} \sum_j \tilde{D}_{21ij}^\alpha , \tag{27b}$$

$$d_{12}^\alpha = N_a S^2 \tfrac{1}{2} \sum_j \tilde{D}_{12ij}^\alpha , \tag{27c}$$

$$d_{22}^\alpha = N_a S^2 \tfrac{1}{2} \sum_j \tilde{D}_{22ij}^\alpha , \tag{27d}$$

and d^γ is defined in (19a). The summations in (27) are over all neighbors of atom i.

The changes in elastic constants in a magnetic field for longitudinal sound waves have been measured for Dy and Ho in the paramagnetic region by Moran and Lüthi.[24] In both cases they found a quadratic dependence on field outside the critical region which they attributed to terms of second order in the strains $\epsilon_{\mu\mu}$ originating either in the exchange coupling or in single-ion terms and depending on a second derivative of the corresponding coupling constant with respect to strain. The results (26) obtained here from the requirement of finite strains likewise vary as H^2 but depend essentially on a first derivative with respect to strain.

An alternative explanation for the longitudinal elastic constants to that of Moran and Lüthi was proposed by Long *et al.*[22] They consider the magnetoelastic coupling as a perturbation carried to second order, within the framework of the usual small-strain formulation. This gives results that depend on the square of the magnetoelastic constants instead of linearly as in Eqs. (26).

From the data of Moran and Lüthi for Dy and Ho we can make a fairly accurate estimate of the combination in curly brackets of Eq. (26a) for $\theta = \frac{1}{2}\pi$, assuming that the present explanation dominates other mechanisms. Using the experimental $\chi(T)$ fitted by a Curie–Weiss law and making use of the relation

$$\Delta c/c = 2\Delta v/v_0 , \tag{28}$$

where v_0 is the sound velocity in zero field in the paramagnetic region, we find the values 0.20×10^{12} ergs/cm^3 for Dy and 2.2×10^{12} ergs/cm^3 for Ho. To obtain these results we used a value of $c_{33} = 0.787\times10^{12}$ ergs/cm^3 for Dy measured by Fisher and Dever[39] at 300 K and a value of $c_{33} = 0.755\times10^{12}$ ergs/cm^3 for Ho from the data of Rosen[44] at 300 K. The value of the two-ion magnetoelastic coupling constant quoted by Pollina and Lüthi[37] for Dy ($DS^2 = 0.2\times10^{12}$ ergs/cm^3) is of the right order of magnitude to account for the value deduced above, but their value for Ho ($DS^2 = 0.14\times10^{12}$ ergs/cm^3) is more than an order of magnitude too small.

From Eqs. (26) it can be seen that it may be possible to deduce separate values for $\frac{3}{5} b_1^\alpha + d_{12}^\alpha$, $\frac{3}{5} b_2^\alpha + d_{22}^\alpha$, d_{11}^α, d_{21}^α, and $\frac{3}{5} b_2^\gamma + d^\gamma$ by carrying out measurements for several different directions of the applied field.

ACKNOWLEDGMENTS

The authors have benefited from discussions with J. Grindlay and correspondence with R. L. Melcher concerning rotational invariance in coupled magnetic and elastic systems.

APPENDIX

In this appendix expressions are given for $|V_{\vec{q}\lambda}|^2$ in terms of the various magnetoelastic and anisotropy constants defined in Eqs. (13) and (22). The direction of magnetization is specified by the angles θ and ϕ. As is implied by the notation $V_{\vec{q}\lambda}$ and $\omega_{\vec{q}\lambda}$, the first subscript gives the direction of propagation of the sound wave while the second specifies its polarization:

$$|V_{aa}|^2 = \frac{E_{\vec{q}} |\hbar\vec{q}|^2}{4\rho\hbar\omega_{aa}} \left(\frac{\{[6 b_1^\alpha m^3 - 2 b_2^\alpha m^3 - b_c^\gamma(\theta)] \sin 2\theta\}^2}{16 N_a S m (A_0 + B_0)} + \frac{[b_s^\gamma(\theta) \sin\theta]^2}{4 N_a S m (A_0 - B_0)} \right) , \tag{A1}$$

$$|V_{bb}|^2 = \frac{E_{\vec{q}} |\hbar\vec{q}|^2}{4\rho\hbar\omega_{bb}} \left(\frac{\{[6 b_1^\alpha m^3 - 2 b_2^\alpha m^3 + b_c^\gamma(\theta)] \sin 2\theta\}^2}{16 N_a S m (A_0 + B_0)} + \frac{[b_s^\gamma(\theta) \sin\theta]^2}{4 N_a S m (A_0 - B_0)} \right) , \tag{A2}$$

$$|V_{cc}|^2 = \frac{E_{\vec{q}} |\hbar\vec{q}|^2}{4\rho\hbar\omega_{cc}} \left(\frac{[(3 b_1^\alpha + 2 b_2^\alpha) m^3 \sin 2\theta]^2}{4 N_a S m (A_0 + B_0)} \right) , \tag{A3}$$

$$|V_{ca}|^2=\frac{E_{\vec{q}}|\hbar\vec{q}|^2}{4\rho\hbar\omega_{ca}}\left(\frac{[b_2^\epsilon m^3\cos 2\theta+f_2(\theta)]^2\cos^2\phi}{4N_a Sm(A_0+B_0)}+\frac{[b_2^\epsilon m^3+f_3(\theta)]^2\cos^2\theta\sin^2\phi}{4N_a Sm(A_0-B_0)}\right), \tag{A4}$$

$$|V_{ac}|^2=\frac{E_{\vec{q}}|\hbar\vec{q}|^2}{4\rho\hbar\omega_{ac}}\left(\frac{[b_2^\epsilon m^3\cos 2\theta-f_2(\theta)]^2\cos^2\phi}{4N_a Sm(A_0+B_0)}+\frac{[b_2^\epsilon m^3-f_3(\theta)]^2\cos^2\theta\sin^2\phi}{4N_a Sm(A_0-B_0)}\right), \tag{A5}$$

$$|V_{cb}|^2=\frac{E_{\vec{q}}|\hbar\vec{q}|^2}{4\rho\hbar\omega_{cb}}\left(\frac{[b_2^\epsilon m^3\cos 2\theta+f_2(\theta)]^2\sin^2\phi}{4N_a Sm(A_0+B_0)}+\frac{[b_2^\epsilon m^3+f_3(\theta)]^2\cos^2\theta\cos^2\phi}{4N_a Sm(A_0-B_0)}\right), \tag{A6}$$

$$|V_{bc}|^2=\frac{E_{\vec{q}}|\hbar\vec{q}|^2}{4\rho\hbar\omega_{bc}}\left(\frac{[b_2^\epsilon m^3\cos 2\theta-f_2(\theta)]^2\sin^2\phi}{4N_a Sm(A_0+B_0)}+\frac{[b_2^\epsilon m^3-f_3(\theta)]^2\cos^2\theta\cos^2\phi}{4N_a Sm(A_0-B_0)}\right), \tag{A7}$$

$$|V_{ba}|^2=\frac{E_{\vec{q}}|\hbar\vec{q}|^2}{4\rho\hbar\omega_{ba}}\left(\frac{[b_s^\gamma(\theta)\sin 2\theta]^2}{16N_a Sm(A_0+B_0)}+\frac{[b_c^\gamma(\theta)+f_3(\theta)]^2\sin^2\theta}{4N_a Sm(A_0-B_0)}\right), \tag{A8}$$

$$|V_{ab}|^2=\frac{E_{\vec{q}}|\hbar\vec{q}|^2}{4\rho\hbar\omega_{ab}}\left(\frac{[b_s^\gamma(\theta)\sin 2\theta]^2}{16N_a Sm(A_0+B_0)}+\frac{[b_c^\gamma(\theta)-f_3(\theta)]^2\sin^2\theta}{4N_a Sm(A_0-B_0)}\right). \tag{A9}$$

For $\sin\theta\neq 0$,

$$\begin{aligned}N_a Sm(A_0+B_0)=&-6b_2m^3P_2^0(\cos\theta)-20b_4m^{10}P_4^0(\cos\theta)-42b_6m^{21}P_6^0(\cos\theta)\\&-6b_6^6m^{21}\sin^6\theta\cos 6\phi\,(1-6\cot^2\theta)+\frac{(b_2^\epsilon m^3)^2\cos^2\theta\,(6\sin^2\theta-1)}{c^\epsilon}+\frac{(b_2^\gamma m^3)^2\sin^2\theta\,(3\sin^2\theta-2)}{2c^\gamma}\\&+\frac{(b_4^\gamma m^{10})^2\sin^6\theta\,(5\sin^2\theta-4)}{4c^\gamma}+\frac{(b_2^\gamma m^3)(b_4^\gamma m^{10})\cos 6\phi\sin^4\theta\,(13\sin^2\theta-10)}{4c^\gamma}\\&+2h_c m\cos\theta-\frac{h_\perp m\cos 2\theta}{\sin\theta}\equiv f_2(\theta)+2h_c m\cos\theta-\frac{h_\perp m\cos 2\theta}{\sin\theta},\end{aligned} \tag{A10}$$

$$\begin{aligned}N_a Sm(A_0-B_0)=&-36b_6^6m^{21}\sin^4\theta\cos 6\phi+\frac{(b_2^\epsilon m^3)^2\cos^2\theta}{c^\epsilon}+\frac{(b_2^\gamma m^3)^2\sin^2\theta}{c^\gamma}+\frac{(b_4^\gamma m^{10})^2\sin^6\theta}{c^\gamma}\\&+\frac{5(b_2^\gamma m^3)(b_4^\gamma m^{10})\cos 6\phi\sin^4\theta}{2c^\gamma}+\frac{h_\perp m}{\sin\theta}\equiv f_3(\theta)+\frac{h_\perp m}{\sin\theta}.\end{aligned} \tag{A11}$$

These two expressions serve to define $f_2(\theta)$ and $f_3(\theta)$. The other quantities appearing in these equations are

$$b_c^\gamma(\theta)=b_2^\gamma m^3\cos 2\phi-b_4^\gamma m^{10}\sin^2\theta\cos 4\phi,\qquad b_s^\gamma(\theta)=b_2^\gamma m^3\sin 2\phi-b_4^\gamma m^{10}\sin^2\theta\sin 4\phi, \tag{A12}$$

$$h_c=N_a g\mu_B H_c S,\qquad h_\perp=N_a g\mu_B(H_a\cos\phi+H_b\sin\phi)S. \tag{A13}$$

When $\sin\theta=0$, the expressions for $f_2(\theta)$ and $f_3(\theta)$ are not valid. Both functions must then be replaced by the function f_1, and Eqs. (A10) and (A11) become

$$N_a Sm(A_0\pm B_0)=-3b_2m^3-10b_4m^{10}-21b_6m^{21}+h_c m=f_1+h_c m. \tag{A14}$$

---

*Work supported by the National Research Council of Canada.

[1]R. A. Toupin, J. Ratl. Mech. Anal. 5, 849 (1956).

[2]H. F. Tiersten, J. Math. Phys. 5, 1298 (1964).

[3]W. F. Brown, Jr., J. Appl. Phys. 36, 994 (1965); *Magnetoelastic Interactions* (Springer–Verlag, New York, 1966).

[4]R. L. Melcher, Phys. Rev. Letters 28, 165 (1972).

[5]R. L. Melcher, Lectures presented at the Enrico Fermi Summer School, Varenna, Italy, 1971 (unpublished).

[6]R. L. Melcher, Phys. Rev. Letters 25, 1201 (1970).

[7]H. A. Buckmaster, Can. J. Phys. 40, 1670 (1962).

[8]E. Callen and H. B. Callen, Phys. Rev. 139, A455 (1965).

[9]D. A. Goodings and B. W. Southern, Can. J. Phys. 49, 1137 (1971).

[10]B. R. Cooper, Phys. Rev. 169, 281 (1968).

[11]H. Marsh and A. J. Sievers, J. Appl. Phys. 40, 1563 (1969).

[12]M. S. S. Brooks, Phys. Rev. B 1, 2257 (1970).

[13]M. Nielsen, H. B. Møller, P. A. Lindgard, and A. R. Mackintosh, Phys. Rev. Letters 25, 1451 (1970).

[14]T. K. Wagner and J. L. Stanford, Phys. Rev. B 5,

1876 (1972).
[15]E. A. Turov and V. G. Shavrov, Fiz. Tverd. Tela 7, 217 (1965) [Sov. Phys. Solid State 7, 166 (1965)].
[16]C. Kittel, Phys. Rev. 110, 836 (1958).
[17]A. I. Akhiezer, V. G. Bar'yakhtar, and M. I. Kaganov, Usp. Fiz. Nauk 71, 533 (1960) [Sov. Phys. Usp. 3, 567 (1961)].
[18]J. Jensen, Intern. J. Magnetism 1, 271 (1971).
[19]D. T. Vigren and S. H. Liu, Phys. Rev. B 5, 2719 (1972).
[20]A. H. Nayyar and D. Sherrington, J. Phys. F. 2, 893 (1972).
[21]S. B. Palmer and E. W. Lee, Proc. Roy. Soc. (London) A327, 519 (1972).
[22]M. Long, A. R. Wazzan, and R. Stern, Phys. Rev. 178, 775 (1969).
[23]L. M. Levinson and S. Shtrikman, J. Phys. Chem. Solids 32, 981 (1971).
[24]T. J. Moran and B. Lüthi, J. Phys. Chem. Solids 31, 1735 (1970).
[25]W. P. Mason, Phys. Rev. 96, 302 (1954).
[26]F. Freyne, Phys. Rev. B 5, 1327 (1972).
[27]H. B. Callen and E. Callen, J. Phys. Chem. Solids 27, 1271 (1966).
[28]J-L. Feron, G. Hug, and R. Pauthenet, *Les Éléments des Terres Rares* (Centre Nationale de la Recherche Scientifique, 1970), Vol. 2, p. 19.
[29]C. D. Graham, Jr., General Electric Report No. 66-C-218, 1966 (unpublished).
[30]M. S. S. Brooks and D. A. Goodings, J. Phys. C 1, 1279 (1968).
[31]C. D. Graham, Jr., J. Appl. Phys. 38, 1375 (1967).
[32]J. J. Rhyne and A. E. Clark, J. Appl. Phys. 38, 1379 (1967).
[33]J. J. Rhyne, S. Foner, E. J. McNiff, Jr., and R. Doclo, J. Appl. Phys. 39, 892 (1968).
[34]R. M. Bozorth, A. E. Clark, and R. J. Gambino, in *Proceedings of the Eleventh International Conference on Low-Temperature Physics, St. Andrews* (St. Andrews Printing Dept., St. Andrews, Scotland, 1968), p. 1106.
[35]R. M. Bozorth, A. E. Clark, and J. H. Van Vleck, Intern. J. Magnetism 2, 19 (1972).
[36]E. S. Fisher and D. Dever, in Proceedings of the Oak Ridge Conference on Rare Earths, 1968 (unpublished), p. 522.
[37]R. J. Pollina and B. Lüthi, Phys. Rev. 177, 841 (1969).
[38]M. Rosen and H. Klimker, Phys. Rev. B 1, 3748 (1970).
[39]E. S. Fisher and D. Dever, Trans. Met. Soc. AIME 239, 48 (1967).
[40]J. Alstad and S. Legvold, J. Appl. Phys. 35, 1752 (1964).
[41]P. de V. Du Plessis, Phil. Mag. 18, 145 (1968).
[42]A. E. Clark, B. F. DeSavage, and R. Bozorth, Phys. Rev. 138, A216 (1965).
[43]B. R. Cooper, Phys. Rev. 169, 281 (1968).
[44]M. Rosen, Phys. Rev. Letters 19, 695 (1967).
[45]J. J. Rhyne and S. Legvold, Phys. Rev. 138, A507 (1965).
[46]J. J. Rhyne, S. Legvold, and E. T. Rodine, Phys. Rev. 154, 266 (1967).
[47]J. J. Rhyne and S. Legvold, Phys. Rev. 140, A2143 (1965).

PHYSICAL REVIEW B VOLUME 7, NUMBER 1 1 JANUARY 1973

Proposal for Notation at Tricritical Points*

Robert B. Griffiths

Department of Physics, Carnegie-Mellon University, Pittsburgh, Pennsylvania 15213

(Received 31 July 1972)

A notation for critical exponents at a tricritical point is proposed on the basis that the line of critical points observed experimentally in metamagnets, NH_4Cl, or He^3-He^4 mixtures defines a special direction in the space of thermodynamic parameters. Scaling at a tricritical point implies certain relations among the exponents which are summarized in a table.

I. INTRODUCTION

At the present time there is a well-developed phenomenological description of ordinary ferromagnetic and liquid-vapor critical points in terms of exponents and scaling,[1] and this phenomenology can be extended fairly easily[2,3] to lines and surfaces of critical points (which arise, for example, in antiferromagnets, fluid mixtures, and liquid He^4) wherever the ideas of "smoothness"[3] or "universality"[4] are applicable. Probably the simplest situation at which smoothness and, hence, the conventional description of critical points breaks down is at a tricritical point,[5] and consequently tricritical points have recently been the subject of several experimental and theoretical investigations.[6-8]

As might be expected a rather diverse notation for tricritical exponents has been employed by different authors. The purpose of this paper is to suggest a notation which is a logical extension to tricritical points of the notation for exponents which is already in use at "ordinary" critical points and at the same time maintains certain essential distinctions which arise at tricritical points and which lead to confusion if ignored. More important, we wish to suggest a point of view closely allied with (and, in fact, an extension of) the geometrical analysis set forth in an earlier paper.[2] Scientists